Flow accelerated corrosion experiment in LBE for corrosion modeling development using impeller equipped facility

Jaewon Choi, Youho Lee*
Department of Nuclear Engineering, Seoul National University, Gwanak-ro 1, Gwanak-gu, Seoul, Korea
jaewon0987@snu.ac.kr

1. Introduction

Lead-cooled Fast Reactor (LFR) is a new concept reactor that improves safety and efficiency by using liquid lead alloys as a coolant. However, modeling development on the effect of high temperature liquid lead coolant on the materials of reactor has still room for improving to universal applicable correlation. As a part of Micro Nuclear Energy Research and Verification Arena (MINERVA) project, the device can control both oxygen concentration and flow rate of LBE (Lead-Bismuth Eutectic) is constructed for corrosion experiment. And this paper covered the process and the results of the first campaign under 400ºC and maximum 3.77 m/s of LBE flow using the experimental device, maintained for 130h to develop corrosion modeling.

2. Theoretical backgrounds

Assuming that the transport flux and dissolution flux of solute have established equilibrium in low oxygen concentration environment, each flux are expressed as follows. (S_M the solubility limit of the solute metal, C_w the concentration of dissolved metal at the wall surface, C_b the concentration of solute in the bulk solution, S the metal/Pb-Bi surface area, K the mass transfer coefficient, and each k_d and k_{pr} the dissolution and precipitation rate coefficient.

$$M_s \underset{k_{pr}}{\overset{k_d}{\rightleftharpoons}} M_d \quad (1)$$

$$\begin{aligned}\vec{\boldsymbol{J}}_{\boldsymbol{diss}} &= \boldsymbol{k_d}[\boldsymbol{M_s}] - \boldsymbol{k_{pr}}[\boldsymbol{M_d}] \\ &= k_{pr}S_M - k_{pr}[M_d] = k_{pr}(S_M - C_w)\end{aligned} \quad (2)$$

$$\vec{J}_T = \frac{1}{S}\frac{dC}{dt} = K(C_W - C_b) \quad (3)$$

$$\vec{J} = \vec{J}_{diss} = \vec{J}_T = R(S_M - C_b),\ \ R = \frac{K\,k_{pr}}{K + k_{pr}} \quad (4)$$

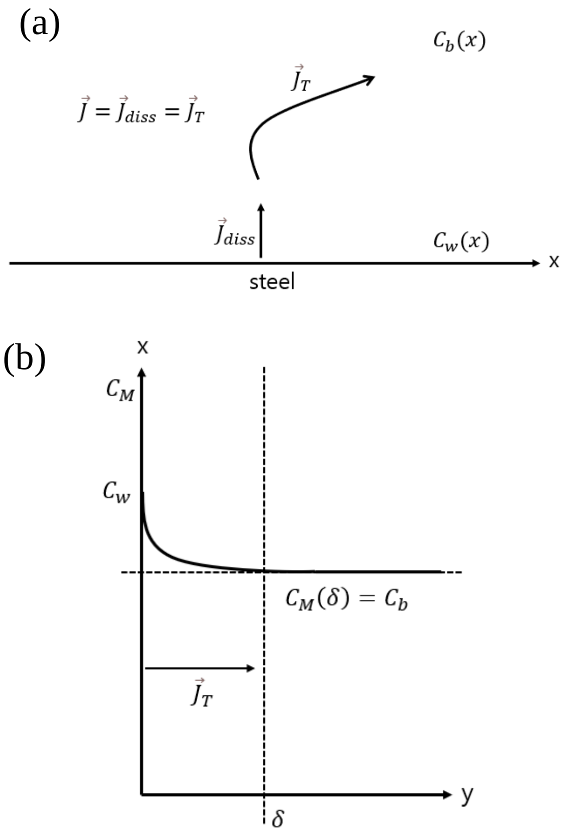

Fig. 1. (a) Presentation of the fluxes governing the dissolution process; (b) iron concentration gradient in the concentration boundary layer. [1]

To establish corrosion modeling, both K depends mainly on T, v and k_{pr} depends on T should be derived under the experiment of constant T and various v, as the dissolution flux (J), the concentration of solute in the bulk solution (C_b), and solubility limit (S_M) can be measured through component analysis after the LBE exposure.

3. Experimental procedure

2.1 Experimental Device for Flow Accelerated Corrosion Using Impeller

Temperature and flow velocity of LBE influence corrosion as mentioned in theoretical backgrounds, dissolved oxygen concentration is also the one of the main factors in modeling as high oxygen concentration forms oxide layer on the material and it slows down the chemical reaction rate with oxygen [2]. So, not only the temperature and flow velocity, but also oxygen concentration should be controlled for the experiment to develop corrosion modeling.

Experimental Device for Flow Accelerated Corrosion Using Impeller is the instrument invented to control temperature, flow rate, and oxygen concentration of LBE which is the main factors effect corrosion (Fig. 2). It designed based on the typical pool-type devices which consist of heater and crucible for stagnant LBE experiment [3]-[5], attaching impeller on the upper part of the instrument. There are two gas port to insert each Ar gas and Ar+4%H2 gas for controlling cover gas and LBE oxygen concentration. And an oxygen sensor purchased from SCK-CEN, Belgium is equipped to measure exact oxygen concentration. The oxygen sensor indicates the electric potential from Bi-Bi_2O_3, and it can be easily calculated to concentration using the equation (5) as follow [6]:

$$E = -3.4756 \times 10^{-1} + 2.5217 \times 10^{-4}\, T - 4.3087 \times 10^{-5}\, T \ln C_o \quad (5)$$

(E: Electric potential (V), T: Temperature (K), C_o : Oxygen concentration in LBE (wt.%))

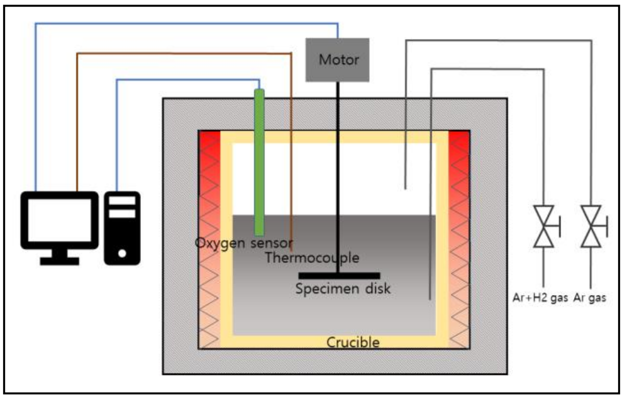

Fig. 2. Schematic figure of newly designed FAC experimental device.

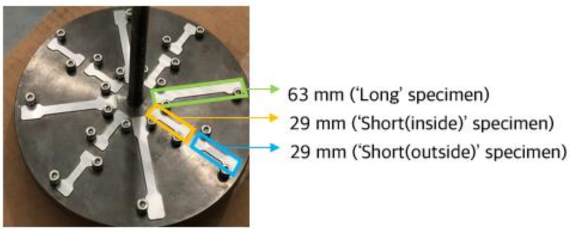

Fig. 3. Actual figure of specimens and specimen holder.

Moreover, specimens are produced dog bone shaped specimen mostly used in tensile test, for easily measuring mechanical properties of material has just been corroded. Also, the specimen holder is designed to fit the specimens correctly. So even if it is the same specimen, it will experience different size of flow rates continuously depending on the distance from the center.

2.2 Experiment conditions and procedure

The material used in the first campaign is SUS 316L which is one of the candidate metals of LFR cladding. Specimens have two types, 63 mm X 10 mm X 1 mm and 29 mm X 10 mm X 1 mm (Fig. 5). Each specimen is designed as shape of dog-bone as mentioned above.

Table I: Conditions of the experiment

Time	133h
Temperature	400℃
Oxygen concentration	$1{\sim}2 \times 10^{-7}$ wt.%
Rotative velocity	400 RPM
Max. linear velocity	3.77 m/s
Pressure	1-1.5 bar

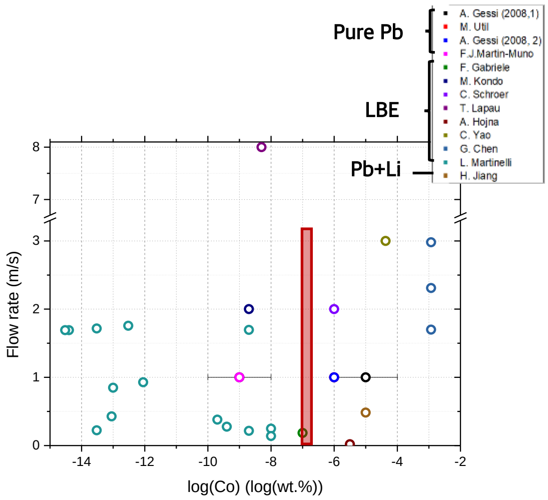

Fig. 4. Comparison in experimental conditions of existing research

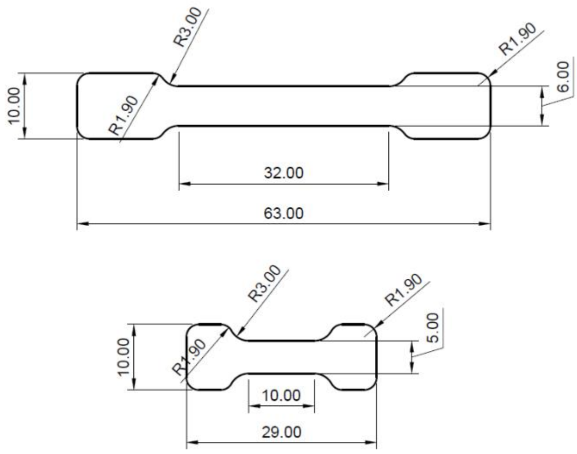

Fig. 5. Sketch of specimens

The condition of the experiment is same as table I. The flow velocity described above is the result that rotative velocity multiplied by diameter of specimen holder. Remained LBE on specimens is removed using ethanol and ultrasonic cleaner at the room temperature, and cleaned specimens was examined by the tensile test and scanning electron microscopy (SEM) and energy-dispersive X-ray spectrometry (EDS).

4. Results and discussion

4.1 The tensile properties of SUS 316L steel

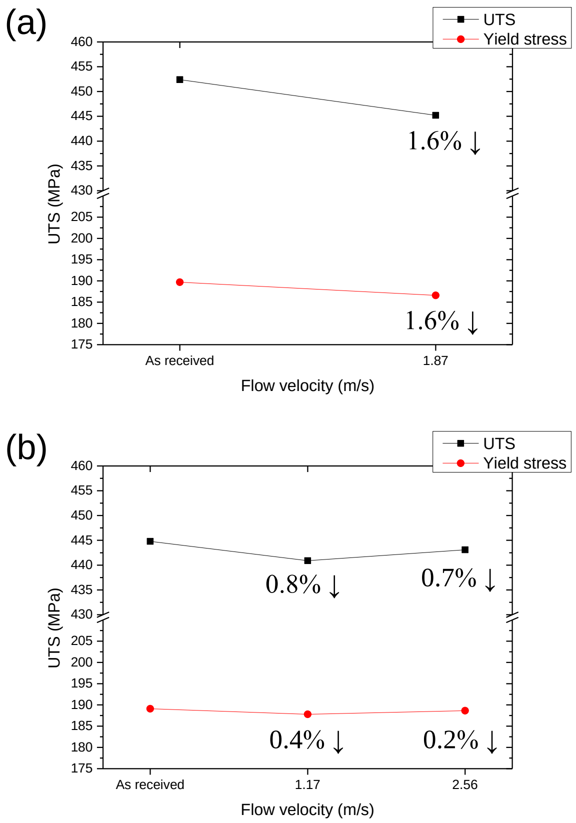

Fig. 6. Changes in ultimate tensile stress (UTS) and yield strength after 133h of LBE exposure
(a): 63 mm (long) specimen, (b): 29 mm (short) specimen

Tensile stresses of specimens were measured at 400 °C and room pressure which is same with the experiment condition. The flow rates specified at fig. 6 (1.17, 1.87, 2.56 m/s) are averaged figure that specimens of different sizes and locations faced. Widths of decrease on UTS and yield stress were not significantly large, considered in error range.

4.2 Changes in composition of matter

Fig. 7 presents SEM images and results of EDS analysis. The composition of matter analyzed on the cross section of the specimens to 250 μm from the surface. As a result, significant change such as formation of oxide layer or decrease in Ni concentration was not found.

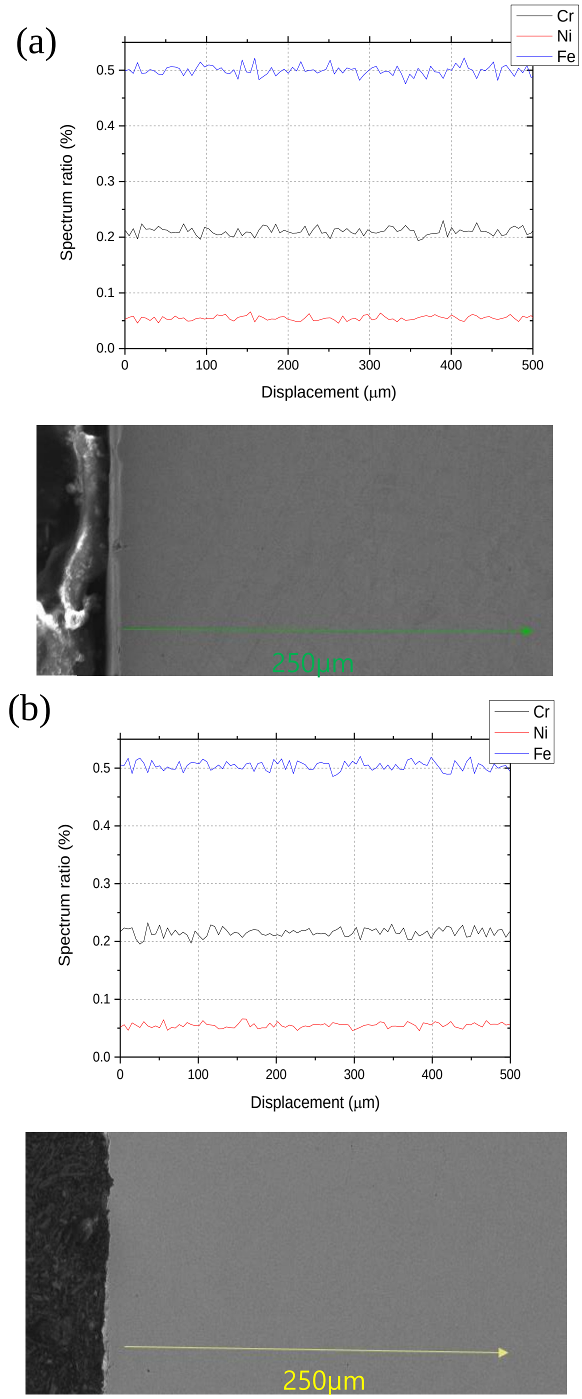

Fig. 7. SEM images and results of EDS analysis of the specimens, (a) as received / (b) exposed by LBE for 130h

5. Conclusions

The first campaign for developing corrosion modeling in LBE flow has been done. Although obvious evidence of corrosion could not be found through the first campaign by the short LBE exposure time, the methodology and the procedure of the experiment could be established. Next campaign is going to be proceeded under hotter (~500 ºC) and less oxygen concentration (~10^{-8}wt.%) condition to observe corrosion. Besides, small-scaled corrosion experiment practiced inside the glovebox is under construction for measuring the exact concentration of solute in the bulk solution and variable control.

REFERENCES

[1], [2] F. Balbaud, and L. Martinelli, 22 - Corrosion Issues in Lead-cooled Fast Reactor (LFR) and Accelerator Driven Systems (ADS), Nuclear Corrosion Science and Engineering, Woodhead Publishing, pp. 831, 2012.

[3] G. Benamati, P. Buttol, V. Imbeni, C. Martini, G. Palombarini, Behaviour of materials for accelerator driven systems in stagnant molten lead, Journal of Nuclear Materials, Vol. 279, Issues 2–3, pp. 308-316, 2000.

[4] A. K. Rivai, M. Takahashi, Compatibility of surface-coated steels, refractory metals and ceramics to high temperature lead–bismuth eutectic, Progress in Nuclear Energy, Vol. 50, Issues 2–6, pp. 560-566, 2008.

[5] E. Yamaki, K. Ginestar, L. Martinelli, Dissolution mechanism of 316L in lead–bismuth eutectic at 500°C, Corrosion Science, Vol. 53, Issue 10, pp. 3075-3085, 2011.

[6] J. Lim, A. Mariën, K. Rosseel, A. Aerts, J. Van den Bosch, Accuracy of potentiometric oxygen sensors with Bi/Bi2O3 reference electrode for use in liquid LBE, Journal of Nuclear Materials, 429, pp. 270-275, 2012.